

Seismic Motion Incoherency Effects on Structure

Dan M. Ghiocel^{*} and Letian Wang^{*}

The paper discusses the effects of seismic wave incoherency on the free-field and structural response motions. Two soil-structure interaction examples including the seismic motion incoherency effects are shown: (i) an axisymmetric nuclear reactor building and (ii) a non-symmetric, L-shaped industrial building with a significant torsional eccentricity. In both examples, the incoherent seismic motion at the foundation level is idealized as a homogeneous and isotropic stochastic field with a given spatial correlation structure. The seismic directional wave passage effects are not included. The two examples show that incoherency effects are significant in the high-frequency ranges. As a result of this, the incoherency effects affect less significantly the low-frequency, overall seismic dynamic responses, namely the base shear and overturning moment, but more significantly the high-frequency vibration modes, and in-structure floor-response spectra. The qualitative effects of motion incoherency are a reduction in the foundation translation excitation, concomitantly with an increase in the foundation torsional excitation, and with slight modifications in the foundation rocking excitation.

INTRODUCTION

The severe effects of nonsynchronous seismic motions, including incoherency and wave passage effects, on structural response of buildings have been repeatedly remarked by post earthquake field observations. Many buildings with high lateral stiffness but with small torsional stiffness suffered significant damages. Typically, the corner columns were heavily damaged. The typical effects of motion incoherency are a reduction in the foundation

^{*} Ghiocel Predictive Technologies Inc., 6th South Main St, 2nd Floor, Pittsford, NY 14534.

translation excitations, concomitantly with an increase in the foundation torsional excitations, and slight modifications in foundation rocking excitation.

In this paper, the same incoherency effects are investigated based on computational incoherent SSI analyses. The seismic incoherent SSI finite element analyses was performed using the ACS SASSI code that includes the capability of considering nonsynchronous stochastic input excitations (including both incoherency and wave passage effects, using either isotropic or an arbitrarily oriented anisotropic coherency structure).

SEISMIC MOTION INCOHERENCY MODELS

Assuming that the seismic wave field, U , can be modeled by a plane wave motion, the cross-spectral density of motion stochastic field for two points i and k , can be expressed by

$$S_{U_i, U_k}(\omega) = [S_{U_i, U_i}(\omega) S_{U_k, U_k}(\omega)]^{1/2} \text{Coh}_{U_i, U_k}(\omega) \quad (1)$$

where $S_{U_i, U_k}(\omega)$ is the cross-spectral density function for point motions U_i and U_k , and $S_{U_j, U_j}(\omega)$, $j = i, k$ is the auto-spectral density for location point j . Inversely, from equation (1), the coherence between the two arbitrary motions can be derived as a complex function of frequency:

$$\text{Coh}_{U_i, U_k}(\omega) = \frac{S_{U_i, U_k}(\omega)}{[S_{U_i, U_i}(\omega) S_{U_k, U_k}(\omega)]^{1/2}} \quad (2)$$

The coherence is a measure of the similarity of the two point motions, including both the amplitude spatial variation and the wave passage effects. Most commonly in engineering applications, the so-called "lagged" coherence is used (Abrahamson et al., 1990). The lagged coherency includes only the amplitude randomness and removes the wave-passage randomness. From physical point of view, the lagged coherence represents the fraction of the total power of seismic motion which can be idealized by a single deterministic plane wave motion called the coherent motion. In the current earthquake engineering language, the lagged coherence is often called simply coherence. More generally than the "lagged" coherence, the "unlagged" coherence includes the wave-passage random effects. The "unlagged" coherence, including both the amplitude spatial variation and wave-passage random effects, is defined in terms of the "lagged" coherence by:

$$\text{Coh}_{U_i, U_k}(\omega) = \text{Coh}_{L, U_i, U_k}(\omega) \exp [i \omega (X_{D,i} - X_{D,j}) / V_D] \quad (3)$$

The term in equation (3) represents the wave passage effect in the direction D, which is expressed in frequency domain by a phase angle between the two motions at two locations with coordinates and in horizontal plane. The parameter is the apparent horizontal seismic wave velocity that is given by the projected distance between the two motion locations on D direction over the horizontal propagation time. Based on the experimental evidence of different records of past earthquakes, and assuming the seismic motion field U is homogeneous, the following analytical forms for the "lagged" coherence function were considered herein is based on Luco-Wong model (Luco and Wong, 1986) defined by

$$\text{Coh}_{L_{U_i, U_k}}(\omega) = \text{Coh}(|X_i - X_j|, \omega) = \exp[-(\gamma\omega|X_i - X_j|/V_s)^2] \quad (4)$$

in which is the coherence parameter and is the shear wave velocity in the soil. The above analytical expression compared with others given in the technical literature based on experiment fitting has the advantage of a theoretical support based on the analytical formulation of shear wave propagation in random media. Luco and Wong, 1986, suggested that the coherence parameter has generic values in the range of 0.10 to 0.30. Using the ACS SASSI code, the "lagged" incoherent motion field can be assumed isotropic or anisotropic. In the last case, the coherence function for the horizontal and vertical motion components can be different. In the horizontal plane the input motion field can be defined as being anisotropic along a predefined direction D arbitrarily oriented. Using a Luco-Wong model, the coherence along the line D is adjusted by changing its parameter. The coherence "adjustment" is based on the relationship:

$$\gamma_D = \gamma(1 - a \cos^2(\alpha_{i,j} - \alpha)) \quad (5)$$

where the parameter a is a scale factor and in the difference is the relative angle between the horizontal line defined by the locations i and j (direction D is defined by these two locations). The scale factor has values between zero and one. A zero value of the scale factor a corresponds to isotropic horizontal motion field, i.e. same coherence parameter for all horizontal directions, while an unit value corresponds to an anisotropic horizontal motion field with coherent motions along the direction D, i.e. cylindrical coherence with a coherence parameter of zero along D.

To implement the stochastic field model of incoherent soil motion, the "lagged" coherence matrix was decomposed using a spectral factorization. Coherence matrix was factorized using the eigen-expansion (Karhunen-Loeve expansion):

$$\text{Coh}_{u_i, u_k}(\omega) = \sum_n^N \lambda_n(\omega) \Phi_n(X_i, \omega) \Phi_n(X_k, \omega) \quad (6)$$

in which λ_n and Φ_n represent the eigenvalues and eigenvectors of the coherence matrix.

ILLUSTRATIVE EXAMPLES

Three case studies on the motion incoherency effects are presented. They show the incoherency effects on (i) in free-field motion, (ii) an axisymmetric structure response and (iii) on non-symmetric L-shaped structure response. The incoherent seismic motion at the foundation level was idealized by a homogeneous stochastic field with an isotropic coherency structure. The input control motion was assumed to be the El Centro NS accelerogram along X axis of the building. No wave passage effects were included.

Free Field Motion

In this example we show results obtained for 500 x 500 square feet free-field surface area. The soil deposit was assumed to be a uniform viscoelastic halfspace with a 1000 fps shear wave velocity. The incoherency motion was computed using the Luco-Wong lagged coherency model in conjunction with the spectral factorization of the coherency kernel. No wave passage was included. Figure 1 shows the incoherency effects on spatial variation of motion amplitude over 500 x 500 square feet area. Figure 2 shows the incoherency motion amplitude amplification factors - that are applied to the control motion amplitude - are plotted in Figure 2 as a function of frequency for two diagonal corners of the investigated surface area (about 700 ft apart). The amplification factors decay significantly over the frequency range from 0 to 20 Hz. For comparison purposes, the average motion was also computed by statistically averaging of the motion amplitudes over the surface grid points. The average motion is extremely smooth when comparing with the local point motions. It should be noted that the wild, fast amplitude oscillations produced by incoherency effects for neighboring frequencies do not impact significantly on the acceleration motion time histories. Figure 3 shows the acceleration time histories computed for the two diagonal corners based on the amplitude amplification factors shown in Figure 2.

Axisymmetric Structure

A reactor building with axisymmetric containment shell and internal structures is considered (Lysmer et al., 1981). Figure 4 shows the free-field soil motion at the interface with the reactor building basemat. The coherence parameter was assumed to be 0.10. The computed coherent and incoherent acceleration amplitude transfer functions and in-structure spectra are compared in Figures 4 and 5. The incoherent SSI analysis results indicate a significant reduction of in-structure floor spectra in high-frequency range, although the incoherency effects for a 0.10 coherence parameter are reduced. These effects indicate that there is possibility to significantly reduce the *design basis* in-structure spectra if we include the motion incoherency effects. Thus, the inclusion of motion incoherency as a design basis procedure will bring significant cost savings by reducing the seismic demand for the internal equipment.

Non-Symmetric Structure

The last example shows the effects of seismic motion incoherency on a non-symmetric L-shaped building with a significant mass eccentricity. The building model shown in Figure 6 represents a typical concrete-steel industrial building sitting on a soft soil deposit with a shear wave velocity of 1000 fps. The foundation consists of isolated foundations under the walls and columns. Motion incoherency effects were computed for a coherence parameter of 0.4, that is quite a large value. Figure 7 and 8 shows the amplitude transfer functions of the acceleration response at the building roof for two opposite diagonal corners. These two roof corners are the roof corner (node 31 in Figure 6b) above the "stiff" concrete part of the building, and the roof corner (node 45 in Figure 6b) above for the "flexible" steel part of the building. The computed transfer functions indicate a large response amplification of motion at the "flexible" corner. The spectral peaks of transfer functions are at different frequencies, 7.83 Hz and 3.90 Hz, due to the nonuniform distribution of the lateral stiffness distribution of the building at the first floor level. The seismic responses in a perpendicular direction of the motion, not shown in here, were significant, indicating a strong torsional response. The spectral peaks of transfer functions at the two roof corners, "stiff" corner (node 31) and "flexible" corner (node 45), were 30% and 60%, respectively, higher for incoherent soil motion than for coherent soil motion. For the base corner column under the "flexible" roof corner (connecting nodes 66 and 69 in Figure 6b) the maximum bending moment increases by approximately 50% due to effects of motion incoherency.

CONCLUDING REMARKS

The paper illustrates that the motion incoherency effects can be either beneficial or unfavorable depending on the configuration and dynamic properties of the building structures. Motion incoherency is favorable for axisymmetric structures, but it could be severely unfavorable for non-symmetric structures with significant mass eccentricities. The last illustrative example of the L-shaped industrial building shows that the effects of motion incoherency increase the bending moments in the corner columns by about 50%. Further future research of these effects of great significance for seismic design is needed before their full implementation in the building design codes will happen.

REFERENCES

- Abrahamson, N.A. et al. (1990). *Spatial Variation of Strong Ground Motion for Use in Soil-Structure Interaction Analyses*, 4th U.S. National Conference on Earthquake Engineering, Palm Springs, May, Vol. 1
- Ghiocel, D.M. (1997). *ACS SASSI/PC - Advanced Computational Software for System Analysis of Soil-Structure Interaction on Personal Computers*, ACS Report, Cleveland, Ohio
- Luco, J. and Wong, H. L. (1986). *Response of a Rigid Foundation to a Spatially Random Ground Motion*, Earthquake Engineering & Structural Dynamics.
- Lysmer, J., Tabatabaie - Raissi, M., Tajirian, F., Vahdani, S., and Ostadan, F. (1981). *"SASSI - A System for Analysis of Soil - Structure Interaction"*, Report No. UCB 81 - 02, Geotechnical Engineering, University of California, Berkeley, April 2.
- Tseng, W.S., Ostadan, F. (1989). *Structure-Soil-Structure Interaction in Different Seismic Environments*, the 10th SMiRT Conference, Vol. K, Los Angeles, California.

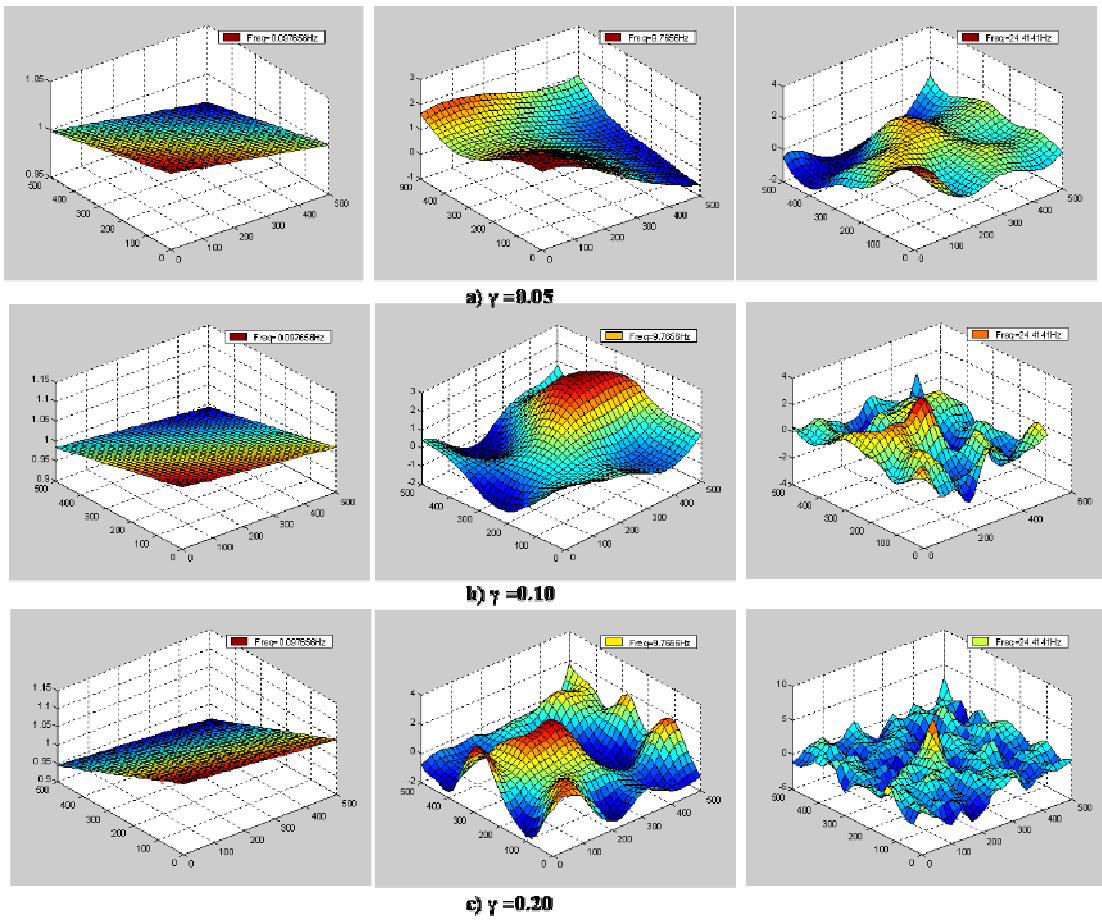


Figure 1. Incoherency Effects on the Spatial Amplitude Variation of Ground Surface Motion at 1, 10 and 20 Hz for Different Coherence Parameter Value: a) 0.05, b) 0.10 and c) 0.20.

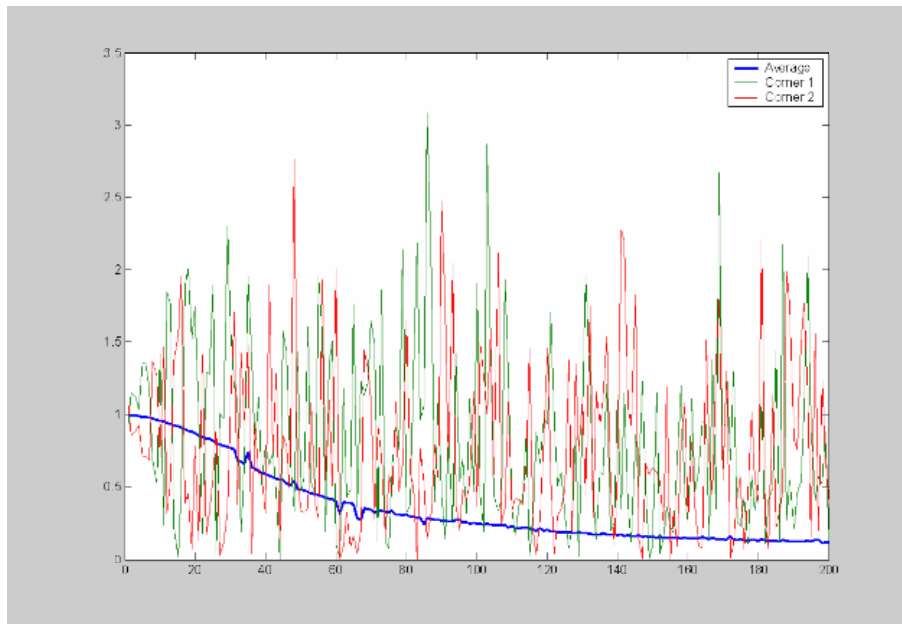


Figure 2. Effects of Seismic Incoherency on Ground Translation - Locally and in Average for A Coherence Parameter of 0.15

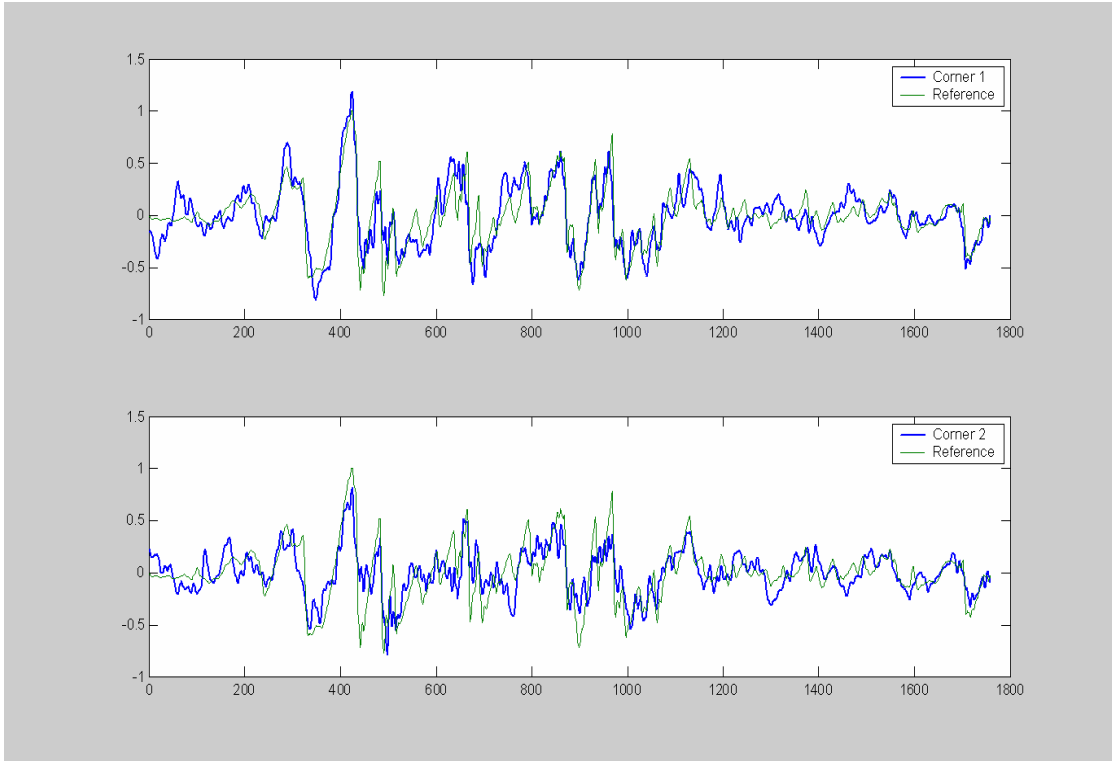


Figure 3. Ground Motions at Two Diagonal Corner Points Separate by 700 ft for A Coherence Parameter of 0.15.

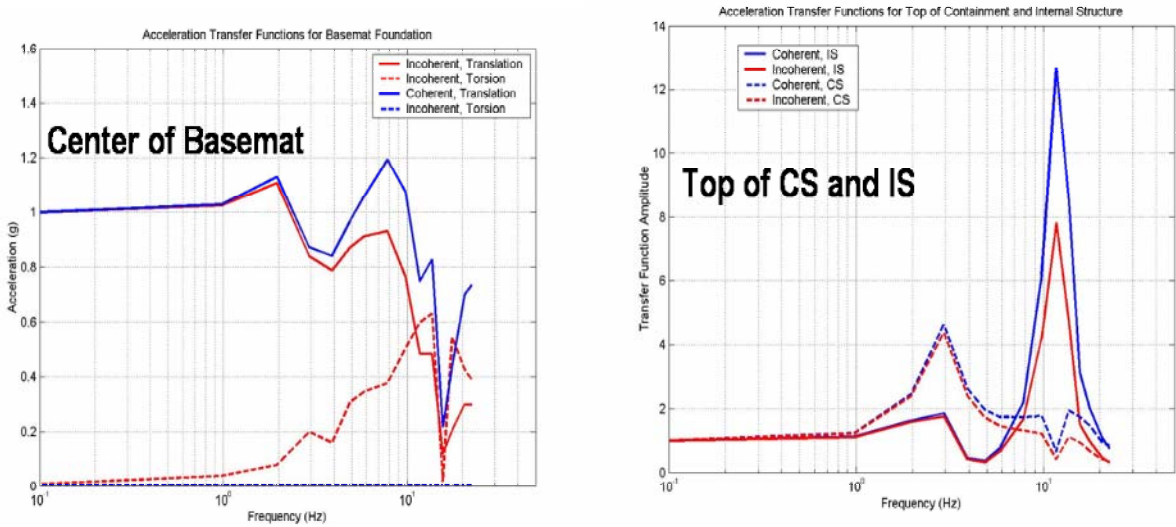


Figure 4. Motion Incoherency Effects on Acceleration Transfer Function Amplitudes

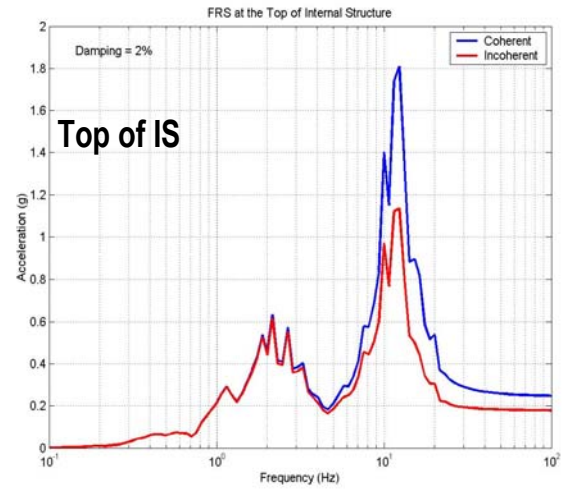
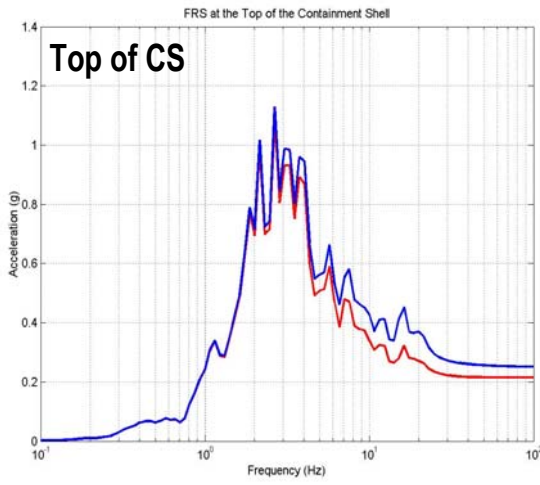


Figure 5. Motion Incoherency Effects on the Seismic In-Structure Floor Response Spectra

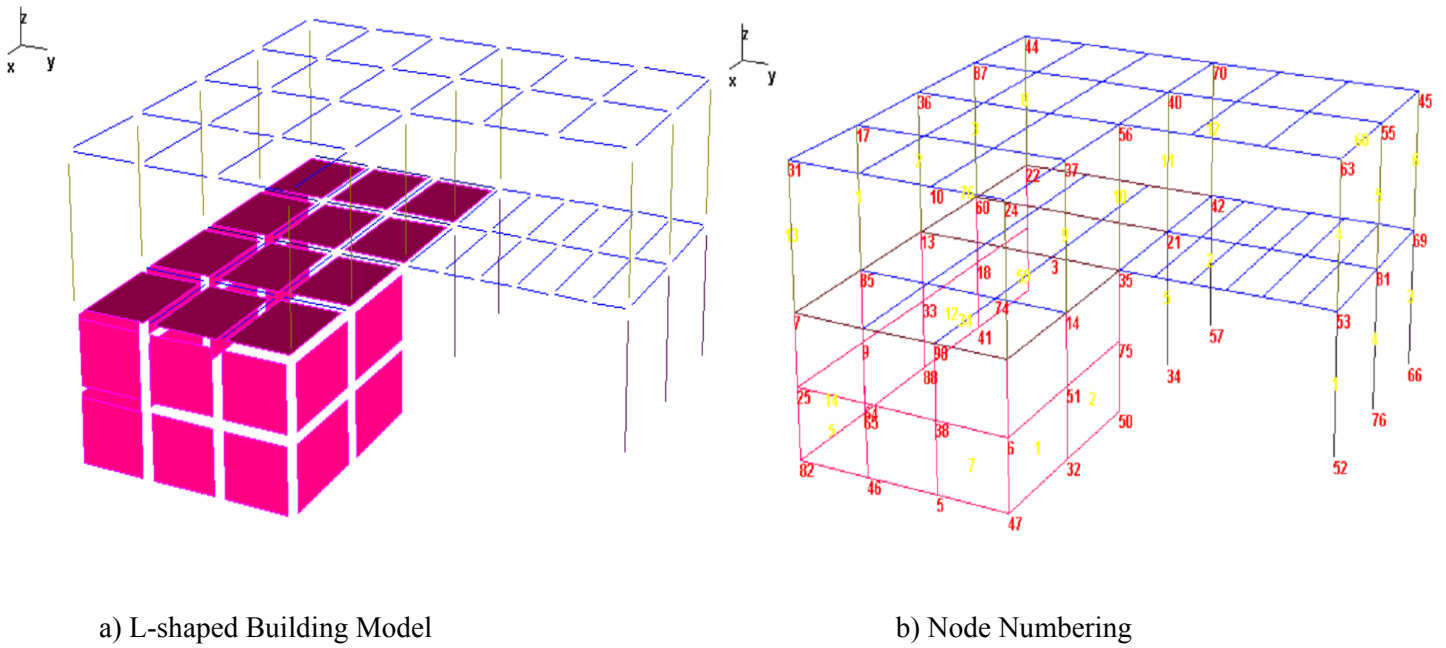


Figure 6. L-shaped Building

**L-SHAPED BUILDING-ROOF CORNER - NODE 31
SEISMIC EXCITATION X DIRECTION**

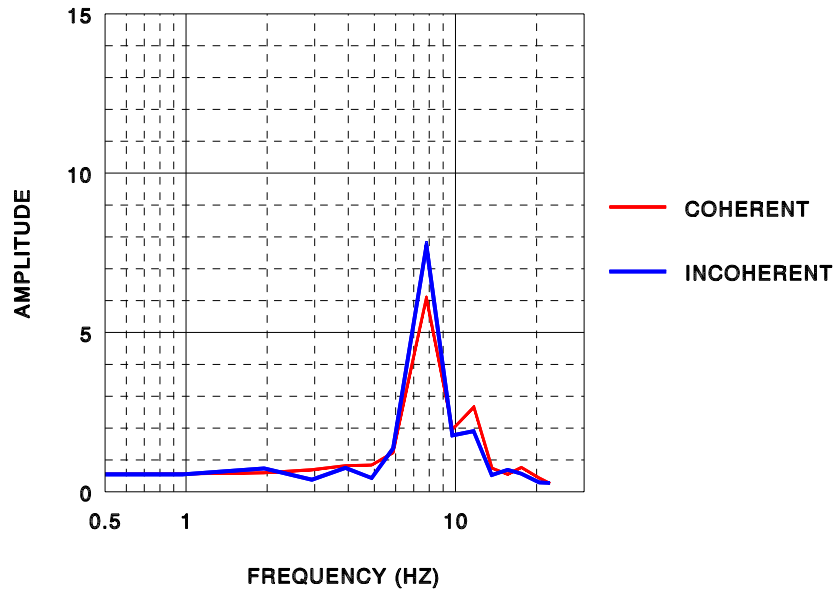


Figure 7. Transfer Function at Node 31

**L-SHAPED BUILDING-ROOF CORNER - NODE 45
SEISMIC EXCITATION X DIRECTION**

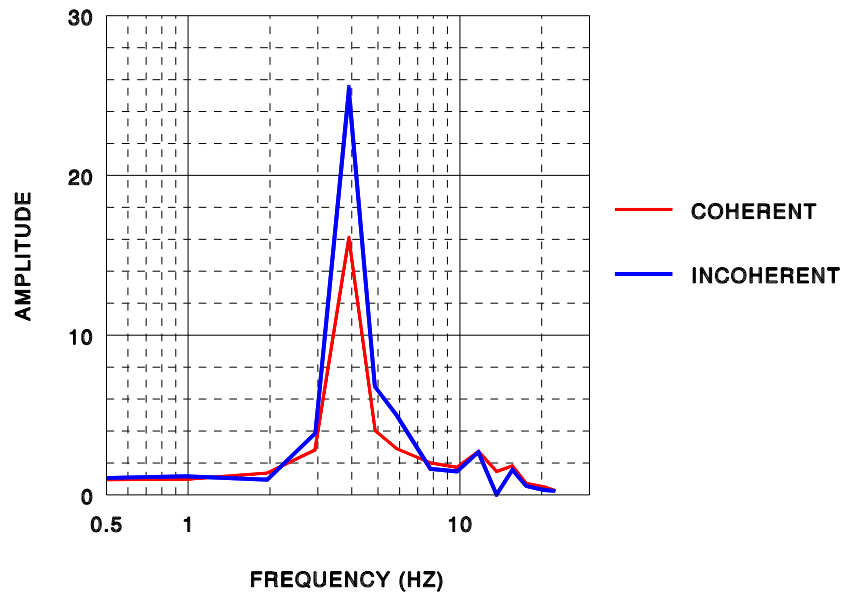


Figure 8. Transfer Function at Node 45